Rock Mech. Rock Engng. (2006) 39 (1), 77–85
DOI 10.1007/s00603-005-0069-0

Rock Mechanics and Rock Engineering
Printed in Austria

Technical Note

The use of Brazilian Test as a Quantitative Measure of Rock Weathering

By

A. Aydin and **A. Basu**

Department of Earth Sciences, The University of Hong Kong, Hong Kong SAR, China

Received March 2, 2005; accepted July 18, 2005
Published online September 23, 2005

Keywords: Brazilian tensile strength, Brazilian deformation index, weathering index, granite.

1. Introduction

Weathering of igneous rocks under humid tropical conditions produces microstructural changes. These begin with discoloration, microfracturing and loosening of grain boundaries, continue with chemical alteration and leaching of constituent minerals, and end with the collapse of relict (skeletal) structure (Aydin and Duzgoren-Aydin, 2002). Microstructural weakening accompanying this process is expected to be dramatic, especially in terms of tensile strength during the early stages of weathering. The behavior of rocks in tension may therefore be an effective indicator of their microstructure, and hence state of weathering. This study explores the potential of diametral stress-strain behavior of igneous rocks in the Brazilian test to scale and predict their degree of weathering. It is shown that the distinct behavioral patterns exhibited by rocks and their initial response expressed by a tangent modulus (named as Brazilian deformation index) are sensitive enough to detect and interpret even minor variations brought about by weathering.

2. Background

The Brazilian tension test (also known as the splitting tensile test) is widely used to evaluate the tensile strength of rocks, as it is easy to prepare and test specimens. Compression-induced extensional fracturing generated in this test is also more

representative of the *in situ* loading and failure of rocks. In the Brazilian tension test, a circular disk placed between two platens is loaded in compression producing a nearly uniform tensile stress distribution normal to the loaded (vertical) diametral plane, leading to the failure of the disk by splitting (Rocco et al., 1999). This tensile stress σ_{t-v} is estimated from the elastic theory (Frocht, 1948):

$$\sigma_{t-v} = \frac{2P}{\pi LD}, \tag{1}$$

where P is load, and L and D are the length and diameter of the disk. Along the horizontal diametral plane, tensile stress (and equivalent strain) values rapidly decrease from a peak level (Eq. (1)) as a function of distance x from the center of the disk:

$$\sigma_{t-h} = \frac{2P}{\pi LD}\left[\frac{D^2 - 4x^2}{D^2 + 4x^2}\right]^2. \tag{2}$$

Equation 2 implies that measurement of the near maximum value of the tensile strain along the horizontal diameter is possible with large diameter specimens and/or short strain gages.

Table 1. Weathering grades, physical properties and Brazilian test results

Sp. No.	WG	D (mm)	L/D	d_g (mm)	ρ_{dry} (gm/cm^3)	n_t (%)	n_e (%)	$\sigma_{t-v(max)}$ (MPa)	*BDI* (GPa)
1	I	83.50	0.32	4.14	2.65	6.15	1.99	10.45	30.40
2	I	83.70	0.34	3.73	2.63	1.71	1.17	9.63	34.38
3	I	84.00	0.32	3.30	2.63	1.46	1.16	9.00	34.46
4	I	83.00	0.30	3.68	2.62	2.10	1.82	9.20	34.26
5	I	83.85	0.44	3.43	2.66	1.31	0.98	10.62	36.43
6	I	83.40	0.47	3.65	2.68	3.76	1.65	6.43	36.48
7	I	83.20	0.26	3.63	2.68	3.75	1.64	10.13	29.77
8	I	83.65	0.36	3.70	2.58	2.49	1.66	10.92	25.14
9	I–II	84.00	0.31	3.73	2.57	3.86	2.86	5.36	20.00
10	I–II	83.80	0.28	3.72	2.63	5.66	1.00	4.22	25.00
11	I–II	60.30	0.44	3.40	2.65	5.06	1.83	7.76	24.35
12	II	60.35	0.31	4.08	2.57	9.00	3.03	5.24	8.88
13	II	83.40	0.35	4.08	2.57	10.91	3.13	3.98	11.90
14	II	60.35	0.37	3.98	2.42	18.23	6.66	3.80	13.33
15	III	83.20	0.32	3.81	2.52	7.35	6.58	1.59	8.00
16	III	83.75	0.35	3.98	2.37	13.87	8.59	2.07	6.67
17	III	83.70	0.30	3.99	2.27	14.54	12.99	1.71	6.25
18	III	83.10	0.36	3.81	2.49	13.00	6.60	1.56	4.21
19	III	83.60	0.33	3.72	2.43	11.62	7.28	2.26	5.00
20	III	83.60	0.29	4.13	2.42	19.21	8.23	1.27	3.89
21	III	83.40	0.31	3.89	2.49	10.70	6.41	2.36	5.88
22	III–IV	83.70	0.32	4.15	2.45	16.30	7.55	1.47	2.05
23	III–IV	83.35	0.40	4.02	2.26	19.71	15.74	1.71	2.70
24	IV	83.70	0.38	4.20	2.13	18.94	18.15	0.97	1.27
25	III–IV	83.00	0.29	2.41	2.55	5.60	4.24	4.54	11.40
26	III–IV	83.30	0.40	2.45	2.56	9.17	4.36	4.56	12.94
27	IV	83.55	0.30	2.32	2.47	5.96	5.52	2.84	8.89
28	IV	83.80	0.32	2.37	2.48	10.39	7.44	2.34	7.59

Abbreviations: WG: weathering grade; D: disk diameter; L: disk length; d_g: average grain size; ρ_{dry}: dry density; n_t: total porosity; n_e: effective porosity under vacuum; $\sigma_{t-v(max)}$: Brazilian tensile strength along vertical (loaded) diametral plane; *BDI*: Brazilian deformational index.

3. Specimens and Test Procedure

The investigation involved the testing of a total of 28 granitic air-dried core specimens of various weathering grades (ranging from Grade I to IV) (Anon, 1995). The specimens (Table 1) were collected from different locations in the Kowloon Granite, a subcircular pluton underlying the most densely populated and central parts of Hong Kong. This intrusive body is remarkably uniform in texture (medium-grained; equigranular) and composition (biotite monzogranite) (Sewell et al., 2000). The diameters and the length-diameter ratios (L/D) of the specimens were within ISRM (1978) and ASTM (2001) specifications (Table 1).

Each specimen was fitted with a 2 cm long strain gage along its horizontal diametral plane, and placed in a custom-built Brazilian test frame with flat bearing blocks (Fig. 1). Loading between flat surfaces was to avoid large variations in the contact areas of the specimens with significantly different stiffness and development of excessively wide contact areas in softer specimens. The loading rate was kept constant at 0.2 kN/s in accordance with the specifications. Compressional loads and corresponding tensile strains were recorded by a data acquisition system (Fig. 1). Post-failure

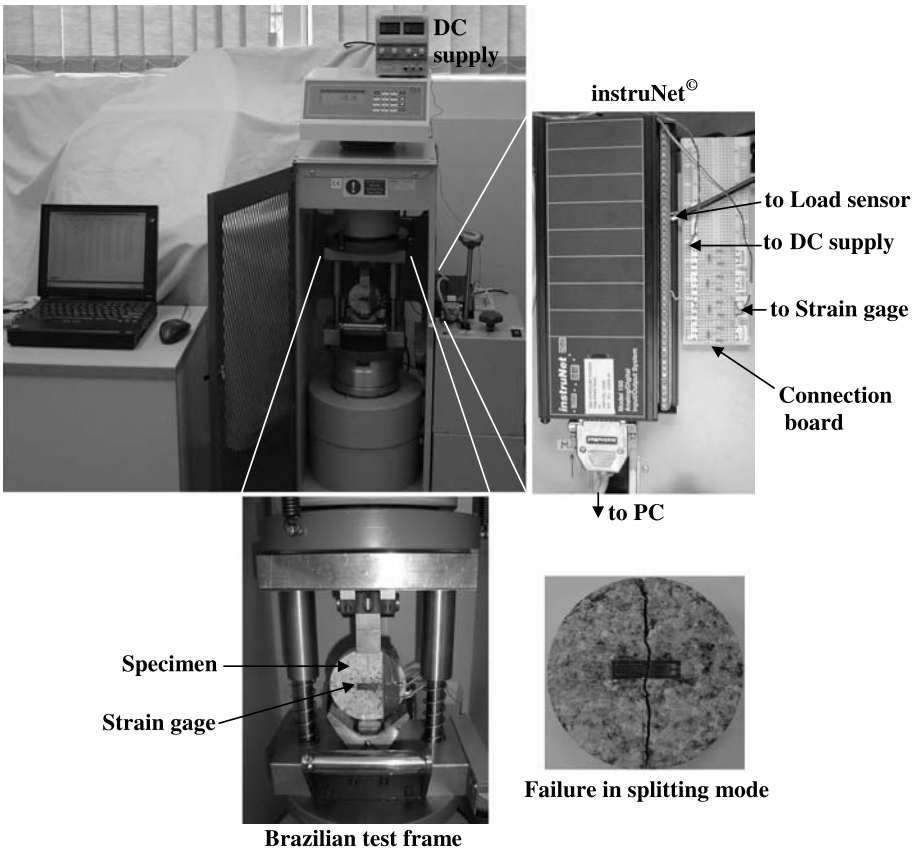

Fig. 1. Brazilian tension test set-up

inspection of the specimens confirmed nearly ideal splitting along their diametral planes (Fig. 1).

4. Results

The tensile stress-strain curves for all test specimens are presented both individually (Fig. 2), and (excluding specimens Nos. 25–28) collectively (Fig. 3). When these

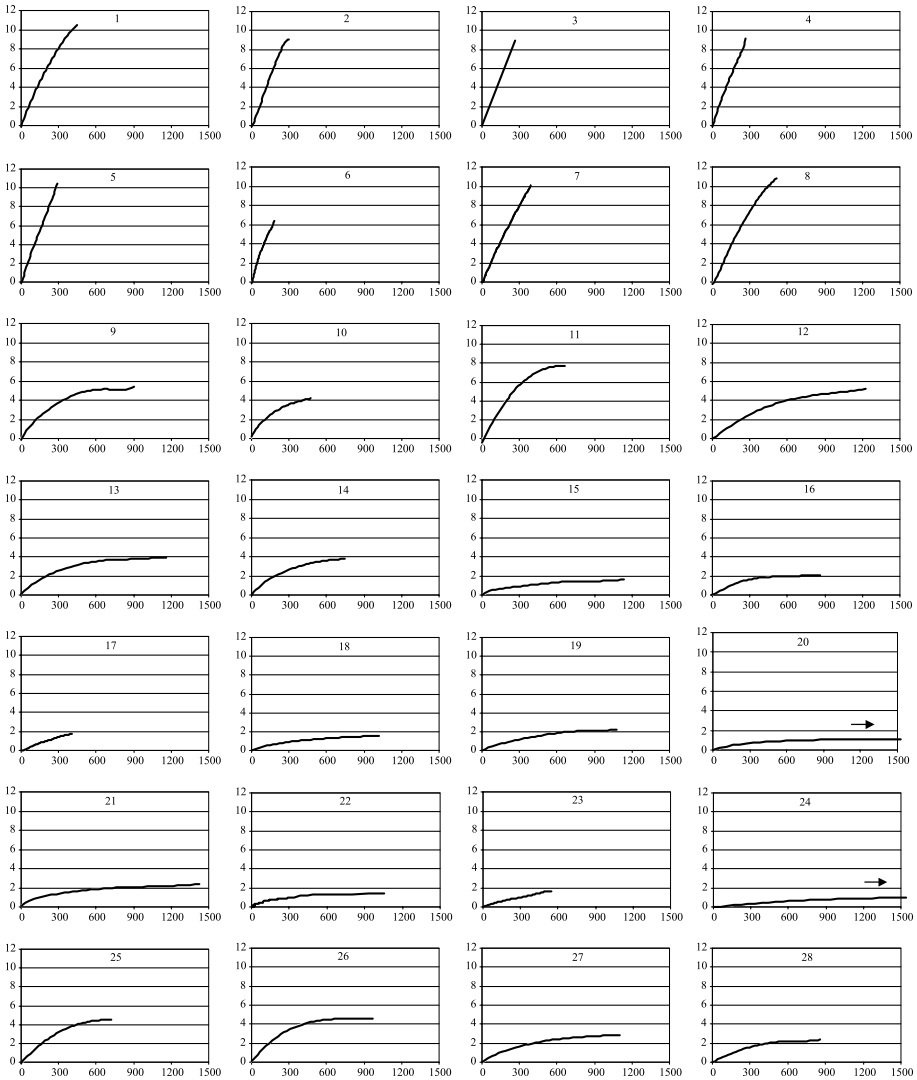

Fig. 2. The tensile stress-strain curves for each specimen

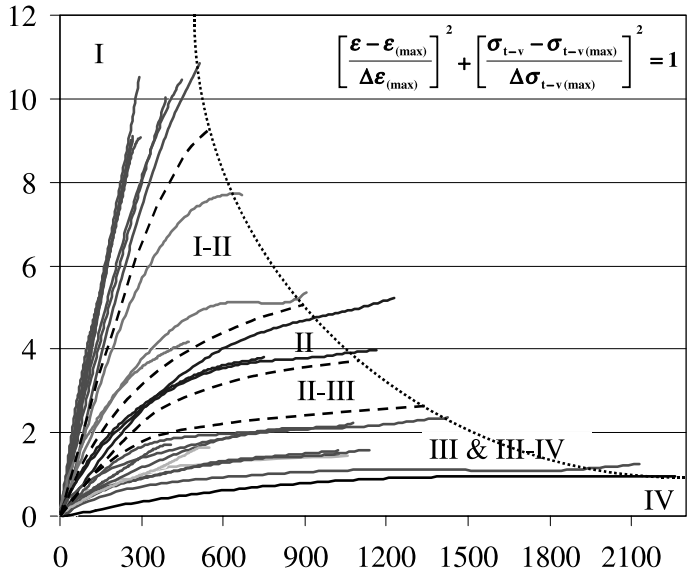

Fig. 3. Behavioral clusters and the generalized pathway for strength and rupture strain variations as a function of weathering

curves are compared with the corresponding weathering grades (Table 1), confirmed by petrographic examination, several distinct behavioral clusters become apparent. The boundaries of these clusters are marked by polynomial curves, shown as dashed lines in Fig. 3. Transformation from linear elastic (over the full stress range) to elastic-plastic behavior takes place suddenly from fresh (Grade I) specimens (Nos. 1–8) to very slightly weathered (Grade I–II) specimens (Nos. 9–11). Obviously, the onset of the weathering process results in considerable changes in the stress-strain behavior, indicating immediate and significant loss of microstructural integrity. The stress-strain patterns continue to show gradual contraction of elastic domain down to Grade IV (Specimen No. 24). Fig. 3 also reveals that decay in tensile strength and increase in rupture strain as a function of weathering follow a roughly identical pathway characterized by a quadratic curve. Thus, basic stress-strain behavior patterns prove to be a powerful graphical tool to identify and interpret even minor changes in degree of weathering in a continuous manner.

Specimen No. 20 (Grade III) was not considered in the above analysis as it bore a peculiar resemblance to Specimen No. 24 (Grade IV). This abnormal behavior may be attributed to the higher density and/or isotropy of its non-interconnected microfractures, as suggested by its high total porosity and large difference between total and effective porosities.

The Brazilian tensile strength $(\sigma_{t-v(\max)})$ values in each of the behavioral clusters overlap with those of the neighboring clusters (Table 1 and Fig. 4). This is not surprising, as the ultimate failure capacity is not only a function of weathering grade but also of the micro-cracks induced during the loading. Logically, therefore, it seems likely that the deformational behavior at the initial stage of loading could be a stronger

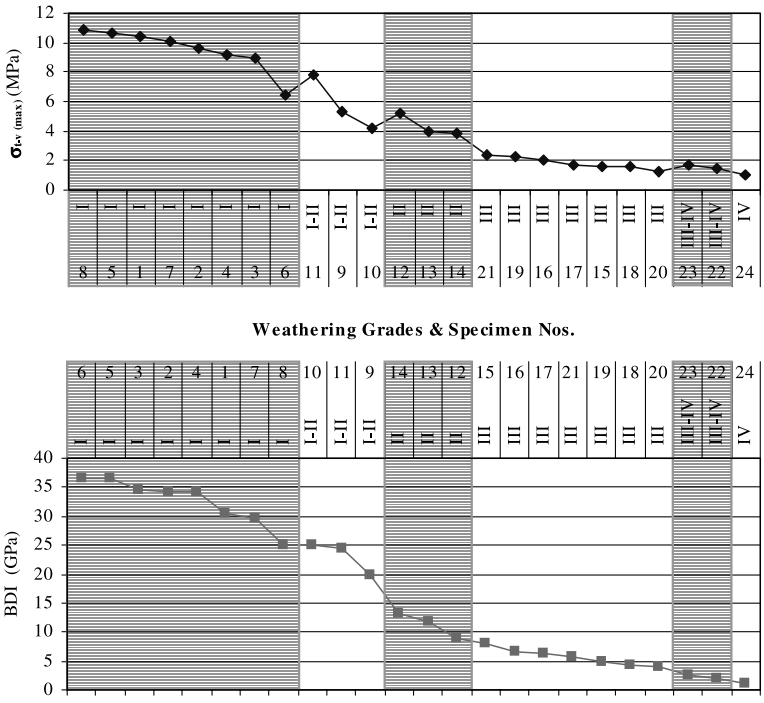

Fig. 4. Trend surfaces of $\sigma_{t-v(\max)}$ and *BDI* with reference to weathering grades. Note that the specimens have been sorted in descending order of each trend parameter

characteristic of that particular weathering grade. The stress-strain ratio (or Brazilian deformational index, *BDI*) of the initial (elastic) response was therefore considered to be a useful means for quantifying weathering-induced changes. Straight lines were visually fitted to the initial linear segment of each curve in order to calculate *BDI*. In contrast to the strength values, no overlaps occurred among the *BDI* values from different weathering grades (Fig. 4), except in the case of Specimens Nos. 25–28. With large differences in its values across the weathering spectrum, *BDI* also offered a much finer resolution than the tensile strength. This suggests that even minor changes in microstructure and weathering grade are accurately reflected by the proposed index.

The average grain size (d_g) of each specimen was determined with the help of the image analysis software analySIS© in order to investigate the influence of grain size on deformational behavior (Table 1). It was noted that the *BDI* values become inconsistent with respect to weathering grades for Specimens Nos. 25–28. Although these four specimens were compositionally similar to the others, they were much finer grained and displayed higher *BDI* values than their coarser grained equivalents. Specimens with significant differences in grain size should therefore be evaluated separately, despite their compositional similarities, to optimize the efficacy of both *BDI* and the other indices used as indicators of weathering grades.

Dry density (ρ_{dry}), effective porosity (n_e), and total porosity (n_t) of the specimens were determined (Table 1) to correlate with corresponding tensile strengths $(\sigma_{t(\max)})$ and the *BDI*. n_e was determined by immersing the specimens into water in a vacuum

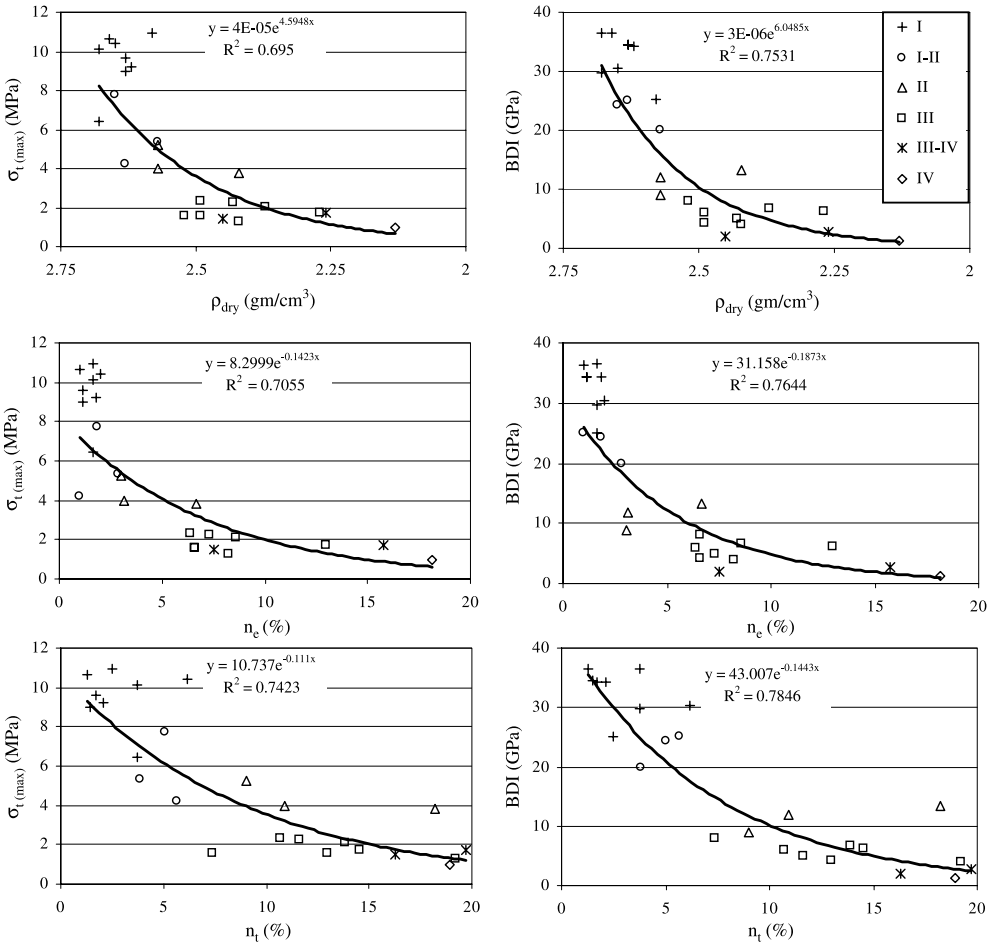

Fig. 5. Correlations of $\sigma_{t-v(\max)}$ and *BDI* with the physical properties

of less than 800 Pa for 1 hr and drying to a constant mass at 105 °C. The water displacement method was adopted to measure the bulk volume of wax-coated weathered samples and the volume of their fine powdered equivalents. ρ_{dry}, n_t and n_e displayed exponential relationships with both $\sigma_{t-v(\max)}$ and the *BDI* (Fig. 5). However, the *BDI* showed significantly better correlation than $\sigma_{t-v(\max)}$, confirming that it is a more reliable index for capturing changes in rock microstructure.

5. Conclusions

The diametral stress-strain behavior of igneous rocks in Brazilian tension test was shown to be a powerful indicator of weathering and accompanying microstructural weakening. In particular,

- specimens that belong to different classes of weathering exhibit distinct behavioral patterns;
- transformation from linear elastic to elastic-plastic behavior develops suddenly from fresh to very slightly weathered specimens, indicating immediate and significant loss of microstructural integrity with the onset of weathering; and
- rates of decay in tensile strength and increase in rupture strain during weathering follow the same pathway, characterized by a quadratic curve.

This sensitivity of the behavioral patterns in the early stages of weathering enables even minor variations brought about by weathering to be identified and interpreted.

The deformational behavior at the initial stage of loading may be considered a reliable indicator of weathering-induced mechanical changes. Accordingly, the tangent modulus (the Brazilian deformational index, *BDI*) expressing the initial (elastic) response of rocks in Brazilian test was proposed to quantify these changes. Unlike the tensile strength values, no overlaps developed among the *BDI* values of the specimens with different weathering grades. Thus, as in the case of behavioral clusters, even minor variations in the microstructural state of igneous rocks are accurately reflected by the proposed index. *BDI* also correlates well with dry density, effective porosity, and total porosity, confirming its suitability for differentiating grades of weathering and for capturing and interpreting the microstructural weakening process. It provides precise and accurate information, of a reliability that cannot be matched by simply studying the physical properties of a specimen. Evidence from studies of physical properties must always be used with caution, as the presence of secondary oxides, the localized interconnectivity of microfractures, and the magnification of small experimental errors can often produce misleading data.

Finally, grain size differences were also shown to have a noticeable influence on deformational behavior. It was demonstrated that evaluating specimens with large grain size differences in separate groups helped to enhance the effectiveness of *BDI* as an indicator of weathering.

Acknowledgements

The work was supported by the Research and Conference Grants Committee of The University of Hong Kong. The authors gratefully acknowledge the technical assistance provided by Mr. Alan Kwok of the Department of Earth Sciences.

References

Anonymous (1995): The description and classification of weathered rocks for engineering purposes: Geological Society Engineering Group Working Party Report QJEG 28, 207–242.

ASTM (2001): Standard test method for splitting tensile strength of intact rock core specimens, Designation D 3967–95a.

Aydin, A., Duzgoren-Aydin, N. S. (2002): Indices for scaling and predicting weathering-induced changes in rock properties. Env. Eng. Geosci. 8, 121–135.

Frocht, M. M. (1948): Photoelasticity, Vol. II. John Wiley, New York.

ISRM (1978): Suggested methods for determining tensile strength of rock materials. Int. J. Rock Mech. Min. Sci. Geomech. Abstr. 15, 99–103.

Rocco, C., Guinea, G. V., Planas, J., Elices, M. (1999): Mechanisms of rupture in splitting tests. ACI Mater. J. 96, 52–60.

Sewell, R. J., Campbell, S. D. G., Fletcher, C. J. N., Lai, K. W., Kirk, P. A. (2000): The pre-Quaternary geology of Hong Kong. Geotechnical Engineering Office, Hong Kong.

Authors' address: Dr. Adnan Aydin, The University of Hong Kong, Department of Earth Sciences, Pokfulam Road, Hong Kong SAR, China; e-mail: aaydin@hku.hk